Path-integral ground state and superfluid hydrodynamics of a bosonic gas of hard spheres

Maurizio Rossi and Luca Salasnich
Dipartimento di Fisica e Astronomia "Galileo Galilei" and CNISM, Università di Padova, Via Marzolo 8, 35122 Padova, Italy
(Received 27 August 2013; published 14 November 2013)

We study a bosonic gas of hard spheres by using the exact zero-temperature path-integral ground-state (PIGS) Monte Carlo method and the equations of superfluid hydrodynamics. The PIGS method is implemented to calculate for the bulk system the energy per particle and the condensate fraction through a large range of the gas parameter na^3 (with n the number density and a the s-wave scattering length), going from the dilute gas into the solid phase. The Maxwell construction is then adopted to determine the freezing at $na^3 = 0.264 \pm 0.003$ and the melting at $na^3 = 0.290 \pm 0.003$. In the liquid phase, where the condensate fraction is finite, the equations of superfluid hydrodynamics, based on the PIGS equation of state, are used to find other relevant quantities as a function of the gas parameter: the chemical potential, the pressure, and the sound velocity. In addition, within Feynman's approximation, from the PIGS static structure factor we determine the full excitation spectrum, which displays a maxon-roton behavior when the gas parameter is close to the freezing value. Finally, the equations of superfluid hydrodynamics with the PIGS equation of state are solved for the bosonic system under axially symmetric harmonic confinement obtaining its collective breathing modes.

DOI: 10.1103/PhysRevA.88.053617 PACS number(s): 03.75.Hh, 03.75.Kk, 02.70.Ss

I. INTRODUCTION

In this paper we analyze a system of identical interacting bosons by using the hard-sphere (HS) model [1], which is a useful reference system for classical and quantum many-body theories both for weak and strong interactions because it depends only on one interaction parameter: the sphere diameter a [1–3]. The quantum HS model has led to the understanding of several general features of helium in its condensed phases [2,3], serving as a reference or a starting point for studies with more accurate potentials [4]. In addition, the quantum HS model provides the standard benchmark for mean-field approaches [5] such as, for example, Gross-Pitaevskii equation or Hartree-Fock-Bogoliubov approximation [6]. A large number of approaches have been put forward to deal with quantum HS and, among them, Monte Carlo method based on Feynman's path integrals come out as a most powerful tool [7]. Path-integral Monte Carlo (PIMC) studies of quantum HS systems at finite temperature cover almost the whole relevant gas parameter range [7–10]. However, at zero temperature, there are studies that cover (with different techniques) only portions of the na^3 range and are mainly devoted to the investigation of different properties such as the universal behavior in the dilute limit [5] or the gas-solid transition [4].

Here we calculate the equation of state of the bulk quantum HS system of identical bosons from very low gas parameter value up to high-density solid with path-integral ground-state (PIGS) Monte Carlo [11] method, which provides exact expectation values on the ground state. Our exact PIGS results for the equation of state are then used to derive other relevant properties by means of the equations of superfluid hydrodynamics [2,3]. Actual experiments on bosonic atomic gases reach so low temperatures that the effects of thermal fluctuations are largely negligible, making a zero-temperature approach well justified [2,3]. The paper is organized in the following way. The basic features of the PIGS method are reported in Sec. II. Numerical results on the ground-state energy and condensate fraction are shown and discussed in Sec. III, where we compare our data with previous Monte Carlo calculations and other theoretical approaches. In Sec. IV we introduce the zero-temperature hydrodynamic equations of superfluids [2,3] and we use them (with the PIGS equation of state) to find other relevant quantities as a function of the gas parameter: the chemical potential, the pressure, and the sound velocity. We find that our sound velocity, which gives the low-momentum linear slope of the excitation spectrum, is in excellent agreement with the numerical results obtained with the help of the PIGS static response function. Moreover, within Feynman's approximation, we determine the full spectrum of elementary excitations, which displays a maxon-roton behavior when the gas parameter is close to the freezing value. In Sec. V we consider the inclusion of an anisotropic but axially symmetric trapping harmonic potential. The collective modes of the confined Bose gas are then easily calculated using again the equations of superfluid hydrodynamics with the PIGS equation of state, which is locally approximated with a polytropic equation of state [12]. The paper is concluded by Sec. VI.

II. PIGS METHOD

The aim of PIGS is to improve a variationally optimized trial wave function ψ_t by constructing, in the Hilbert space of the system, a path which connects the starting ψ_t with the exact lowest-energy wave function of the system, ψ_0, constrained by the choice of the number of particles N, the geometry of the simulation box, the boundary conditions, and the density n, provided that $\langle \psi_t | \psi_0 \rangle \neq 0$. The correct correlations among the particles arise during this path through the action of the imaginary time evolution operator $\hat{G} = e^{-\tau \hat{H}}$, where $\hat{H}$ is the Hamiltonian operator. In principle, ψ_0 is reached in the limit of infinite imaginary time, but a very accurate representation for ψ_0 is given by $\psi_\tau = e^{-\tau \hat{H}} \psi_t$, if τ is large enough (but finite).

The wave function ψ_τ can be analytically written by discretizing the path in small imaginary time steps. This discretization is necessary since the available approximations

for $\hat{G}$ became more accurate as the imaginary time step goes smaller [13]. Here we have used the Cao-Berne approximation [14], which is one of the most efficient propagators (i.e., allows for larger values of imaginary time step) for HS [9]. Because of this discretization of the imaginary time path, the quantum system is mapped into a system of specially interacting classical open polymers [11]. Each open polymer represents the full imaginary time path of a quantum particle that is sampled by means of the Metropolis algorithm. Thus the entire imaginary time evolution of the system is sampled at each Monte Carlo step [15].

An appealing feature of the PIGS method is that, in ψ_τ, the variational ansatz acts only as a starting point, while the full path is governed by $\hat{G}$, which depends only on the Hamiltonian $\hat{H}$. Thus the PIGS method turns out to be unbiased by the choice of the trial wave function [15] and then the only input is $\hat{H}$. In the coordinate representation, the Hamiltonian of the quantum HS system is

$$H = -\frac{\hbar^2}{2m}\sum_{i=1}^{N}\nabla_i^2 + \sum_{\langle i,j\rangle} V(r_{ij}), \tag{1}$$

where $r_{ij} = |\vec{r}_i - \vec{r}_j|$ and

$$V(r) = \begin{cases} +\infty & \text{for} \quad r < a, \\ 0 & \text{otherwise.} \end{cases} \tag{2}$$

The Hamiltonian (1) can be reduced in a useful adimensional form by giving the energies in units of $\frac{\hbar^2}{2ma^2}$ and the lengths in units of a, which represents also the s-wave scattering length. We make use of these reduced units throughout the paper.

The trial wave function ψ_t does not really need to be fully variational optimized: in fact, for a large enough value of τ, PIGS results turn out to be independent on ψ_t, in both the phases [15,16]. The sole role of ψ_t is to determine the length of the path in imaginary time [15] to converge on ψ_0: the better is ψ_t, the faster is the convergence. Here, as ψ_t, we have employed a Jastrow wave function, where the two-body correlations are given by the first-order expansion of the exact solution for the two-body problem, i.e.,

$$\psi_t(R) = \prod_{\langle i,j\rangle}\left(1 - \frac{a}{r_{ij}}\right), \tag{3}$$

where $R = \{\vec{r}_1, \ldots, \vec{r}_N\}$ are the coordinates of the N HS.

All the approximations involved in the PIGS method, i.e., the choice of the total imaginary time τ and of the imaginary time step $\delta\tau$ (that fixes the quality of the approximation on $\hat{G}$), are so well controlled that the resulting systematic errors can be reduced within the unavoidable Monte Carlo statistical error. In this sense PIGS is an exact $T = 0$ K method [11,15].

In order to improve the ergodicity of the Monte Carlo sampling, we have implemented bosonic permutations [17], even if not required in principle since (3) has the correct Bose symmetry, and a canonical (i.e., with fixed N) version of the worm algorithm [18], which has the ulterior advantage of giving access also to off-diagonal properties within the same simulation.

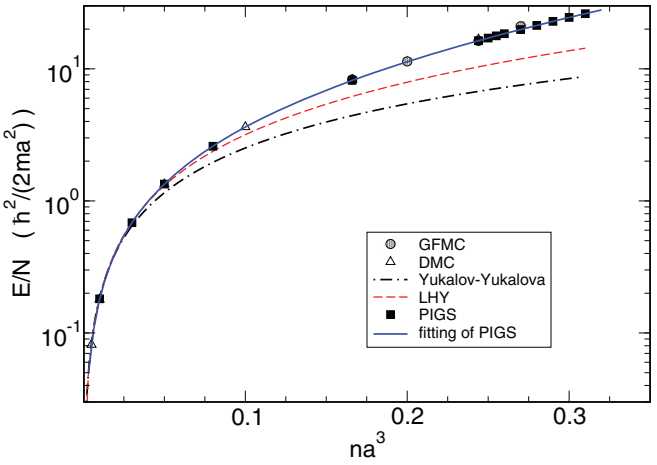

FIG. 1. (Color online) Energy per particle E/N in units of $\hbar^2/2ma^2$ in the gas phase as a function of the gas parameter na^3 computed with PIGS (filled squares) compared with previous GFMC [4] (shaded circles) and DMC [5] (open triangles) results. Error bars are smaller than the used symbols. Dashed line: LHY perturbative approach [19]; dot-dashed line: Yukalov-Yukalova improved perturbative approach [21]; solid line: fit of PIGS data.

III. GROUND-STATE ENERGY AND CONDENSATE FRACTION

We have studied with PIGS a system of $N = 256$ HS in a cubic box with periodic boundary conditions in all the directions, for values of the gas parameter na^3 ranging from dilute gas, namely $na^3 = 10^{-3}$, up to $na^3 = 0.5$, deep inside the solid phase. By studying the convergence in τ and $\delta\tau$ of the energy per particle we have fixed the values $\tau = 0.225\ 2ma^2/\hbar^2$ and $\delta\tau = 0.015\ 2ma^2/\hbar^2$ to be a very good compromise between accuracy and computational cost. For some values of na^3, we have checked the convergence of our results both by reducing the time step to $\delta\tau = 0.005\ 2ma^2/\hbar^2$ and by extending the total projection time up to $\tau = 0.245\ 2ma^2/\hbar^2$. We have performed also simulations with $N = 400$ and $N = 500$ HS in order to verify the presence of size effects, especially close to the gas-solid transition region. We find that the energy per particle does not sensibly change within the error bars, inferring that our results are not affected by a significant size effect.

Our results for the energy per particle E/N as a function of the gas parameter are reported in Fig. 1. We find an excellent agreement with previous GFMC [4] and DMC data [5] in the range of gas parameter values covered by the previous studies. We report also two mean-field predictions for E/N: the perturbative correction to the Bogoliubov mean-field due to Lee, Huang, and Yang (LHY) [19] that turns out to be in a quite fair good agreement with Monte Carlo data up to $na^3 \simeq 5 \times 10^{-2}$ [20], and a more recent perturbative approach due to Yukalov and Yukalova [21] that, however, distances itself from Monte Carlo data for just lower values of na^3.

By adding successive powers at the mean-field prediction of Bogoliubov with the LHK perturbative correction, we have fit our data with the expression [20]

$$\frac{E}{N} = \frac{\hbar^2}{2ma^2} f_g(na^3), \tag{4}$$

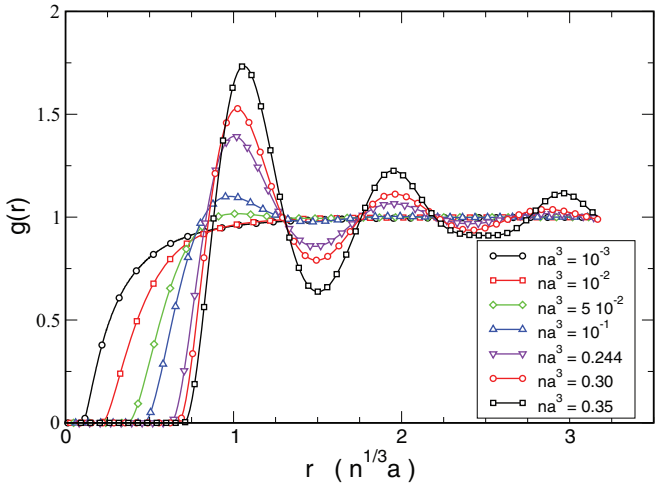

FIG. 2. (Color online) Pair-correlation function $g(r)$ for different values of the gas parameter na^3 computed with PIGS. Error bars are smaller than the used symbols.

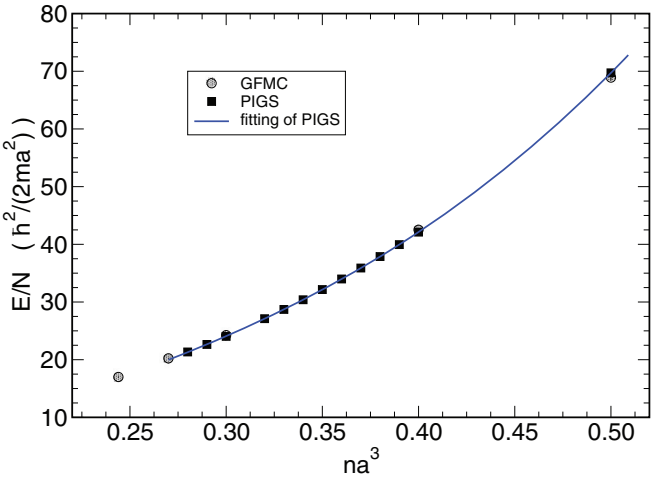

FIG. 3. (Color online) Energy per particle E/N in units of $\hbar^2/2ma^2$ in the solid phase as a function of the gas parameter na^3 computed with PIGS (filled squares) compared with previous GFMC [4] (shaded circles) results. Error bars are smaller than the used symbols. Solid line: fit of PIGS data.

where

$$f_g(x) = 4\pi x\left(1+\frac{128}{15\sqrt{\pi}}\sqrt{x}\right) + a_2x^2\ln(x) + b_2x^2 + a_{5/2}x^{5/2}\ln(x) + b_{5/2}x^{5/2}. \quad (5)$$

The best values for the parameters coming from the fit of the PIGS data are $a_2 = 145.5$, $b_2 = 842.8$, $a_{5/2} = 422$, and $b_{5/2} = -492$. The resulting curve of $f_g(x)$ is also reported as a solid line in Fig. 1.

By increasing the gas parameter the system spontaneously breaks the translational invariance due to the effect of the increased correlations among the particles, resulting in a solid phase, as inferred also from the characteristic oscillations in the pair-correlation function

$$g(r) = \frac{N(N-1)}{n^2}\frac{\int\prod_{j=3}^{N}d\vec{r}_j|\psi_0^*(\vec{r},0,\vec{r}_3,\ldots,\vec{r}_N)|^2}{\int\prod_{j=1}^{N}d\vec{r}_j|\psi_0^*(\vec{r}_1,\vec{r}_2,\ldots,\vec{r}_N)|^2} \quad (6)$$

reported in Fig. 2. The emerging crystal is the FCC, that is the lattice that best fits the cubic geometry of the simulation box. Very recent PIMC simulations [7] have shown, however, that the free-energy difference between the two closed-packed crystals, FCC and HCP, for the quantum HS, is vanishing small. This is not surprising since the difference in these two lattices arises from the second shell of neighbors, and the HS potential is short ranged. In Fig. 3 we report the resulting energy per particles E/N as a function of the gas parameter. Even in this case, we find a quite good agreement with older GFMC data [4]. We find that our results can be well fitted with a standard third-order polynomial [22]

$$\frac{E}{N} = \frac{\hbar^2}{2ma^2}f_s(na^3), \quad (7)$$

where

$$f_s(x) = E_0 + Ax + Bx^2 + Cx^3, \quad (8)$$

and the best values for the fit parameters are $E_0 = -9.33$, $A = 132.6$, $B = -253.6$, and $C = 609.1$. The resulting $f_s(x)$ is plotted as a solid line in Fig. 3.

By using the polynomial fit to the PIGS data (5) and (8) it is possible to locate the transition region between the gas and the solid phase via the standard Maxwell (double tangent) construction. We find that the coexistence region is bounded by $n_fa^3 = 0.264 \pm 0.003$ (freezing gas parameter) and $n_ma^3 = 0.290 \pm 0.003$ (melting gas parameter). These values are close, but not perfectly compatible, with the older GFMC results [4] $n_fa^3 = 0.25 \pm 0.01$ and $n_ma^3 = 0.27 \pm 0.01$. The shift to higher values for the bounding gas parameters can be due to a greater accuracy of the imaginary time propagator used here [7]. Another source of difference can be the strong dependence of such bounding values on the different used fitting formula, even if the energies E/N obtained with the two exact Monte Carlo methods are very close (as one expects from exact techniques).

The worm algorithm [18] give direct access also to the one-body density matrix,

$$\rho_1(\vec{r},\vec{r}') = \int\prod_{j=2}^{N}d\vec{r}_j\psi_0^*(\vec{r},\vec{r}_2,\ldots,\vec{r}_N)\psi_0(\vec{r}',\vec{r}_2,\ldots,\vec{r}_N), \quad (9)$$

that in a uniform system turns out to be a function only of the difference $|\vec{r}-\vec{r}'|$. ρ_1 is the Fourier transform of the momentum distribution of the system; then a finite plateau in the large distance tail of ρ_1 means a Dirac δ in the zero momentum state, i.e., a macroscopic occupation of a single-particle quantum state that is the Bose-Einstein condensation. The condensate fraction n_0/n turns out to be equal to the limiting value of the tail of the one-body density matrix. We plot our results for n_0/n in Fig. 4. In the solid phase the condensate fraction turns out to be zero, in agreement with what is found in ^{4}He systems [16,18]. In the gas phase, even for the condensate fraction we find a satisfactory agreement with previous DMC results [5] in the na^3 range where they were available. Our data confirm that the Bogoliubov prediction overestimates the condensate fraction for a gas parameter larger than $na^3 \simeq 10^{-3}$ [5]. The improved

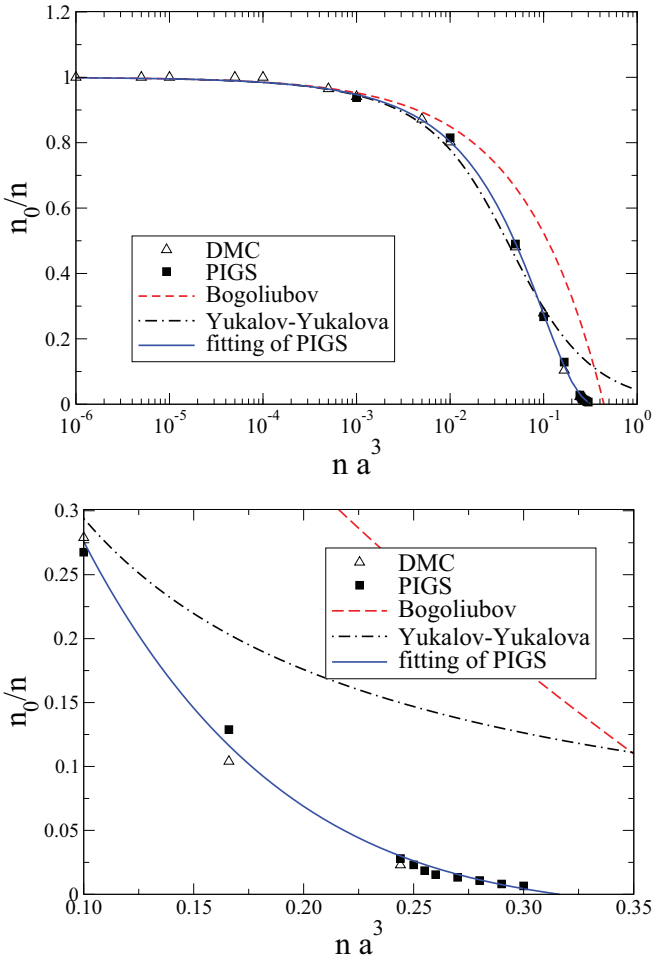

FIG. 4. (Color online) Upper panel: condensate fraction n_0/n as a function of the gas parameter na^3, computed with PIGS (filled squares) compared with the previous DMC results [5] (open triangles). Error bars are smaller than the used symbols. Dashed line: Bogoliubov formula; dot-dashed line: Yukalov-Yukalova improved perturbative approach; solid line: fit of PIGS data. Lower panel: zoom of the upper panel showing DMC and PIGS data in the region where the condensate fraction is going to zero and perturbative methods fail.

perturbative approach of Ref. [21] gives a better prediction of n_0/n starting to overestimate the condensate fraction for values of the gas parameter larger than 10^{-1}, as shown in Fig. 4. To provide an analytical expression for the condensate fraction as a function of the gas parameter, we follow Ref. [20] and fit our data with the formula

$$\frac{n_0}{n} = \Xi(na^3), \tag{10}$$

where

$$\Xi(x) = 1 - \frac{8}{3\sqrt{\pi}}\sqrt{x} - c_1 x - c_{3/2}x^{3/2} - c_2 x^2 - c_{5/2}x^{5/2}. \tag{11}$$

The best values for the fit parameters are $c_1 = 5.49$, $c_{3/2} = -7.86$, $c_2 = -9.52$, and $c_{5/2} = 13.65$.

IV. SUPERFLUID HYDRODYNAMICS AND ELEMENTARY EXCITATIONS

The advantage of a functional parametrization $f_g(x)$, Eq. (5), of the ground-state energy E of the bosonic gas is that it allows straightforward analytical calculations of several physical properties [12]. For example, the bulk chemical potential μ is given

$$\mu = \frac{\partial E}{\partial N} = \frac{\hbar^2}{2ma^2}[f_g(x) + x f_g'(x)], \tag{12}$$

as found by using Eqs. (7) and (5) and taking into account that $x = na^3$ and $\partial x/\partial n = x/n$, while the bulk pressure P reads

$$P = n^2 \frac{\partial}{\partial n}\left(\frac{E}{N}\right) = \frac{\hbar^2}{2ma^2} n x f_g'(x). \tag{13}$$

Moreover, the collective dynamics of our bosonic gas of HS with local density $n(\mathbf{r},t)$ and local velocity $\mathbf{v}(\mathbf{r},t)$ can be described by the following zero-temperature hydrodynamic equations of superfluids [2,3],

$$\frac{\partial n}{\partial t} + \nabla \cdot (n\mathbf{v}) = 0, \tag{14}$$

$$m\frac{\partial \mathbf{v}}{\partial t} + \nabla\left[\frac{1}{2}mv^2 + \mu[n,a]\right] = \mathbf{0}, \tag{15}$$

where $\mu[n,a]$ is the bulk chemical potential, given by Eq. (12). These equations describe a generic fluid at zero temperature which is inviscid (zero viscosity) and irrotational ($\mathbf{v} \wedge \mathbf{v} = \mathbf{0}$) [2,3]. The irrotationality implies that $\mathbf{v} = \nabla\theta$, where $\theta = \theta(\mathbf{r},t)$ is a scalar field which must be an angle variable to get the quantization of the circulation of the velocity [2,3]. Thus, from the knowledge of the bulk equation of state (12) one can study the collective superfluid dynamics of the system by solving Eqs. (14) and (15). In particular, we are interested in the propagation of sound waves in the superfluid. In this case, by taking into account a small $\delta n(r,t)$ variation of the local density with respect to the uniform value n and linearizing the hydrodynamic equations, one finds the familiar wave equation

$$\left[\frac{\partial^2}{\partial t^2} - c_s^2\nabla^2\right]\delta n(\mathbf{r},t) = 0, \tag{16}$$

where c_s is the sound velocity, given by

$$mc_s^2 = n\frac{\partial \mu}{\partial n} = \frac{\hbar^2}{2ma^2}[2x f_g'(x) + x^2 f_g''(x)]. \tag{17}$$

It is well known that this wave equation admits monochromatic plane-wave solutions, where the frequency ω and the wave vector $\mathbf{k}$ are related by the phononic dispersion formula

$$\hbar\omega(k) = c_s\hbar k, \tag{18}$$

where $k = |\mathbf{k}|$ is the wave number. In Fig. 5 we plot the bulk chemical potential μ, the bulk pressure P, and the sound velocity c_s as a function of the gas parameter na^3. All these physical quantities are calculated on the basis of the parametrization (7) and (5) of the PIGS energy E.

The zero-temperature equations of superfluid hydrodynamics (14) and (15), equipped by the constitutive equation of state (12) which is based on the parametrization (7) and (5) of the PIGS energy, give reliable information only on the low

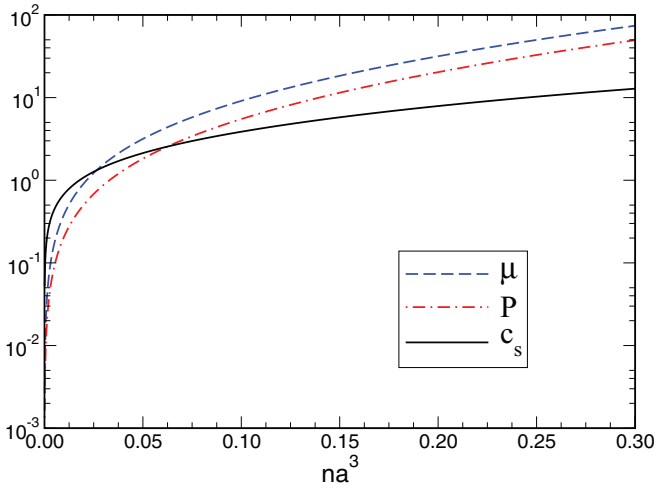

FIG. 5. (Color online) Various physical quantities as a function of the gas parameter na^3: the bulk chemical potential μ [in units of $\hbar^2/(2ma^2)$], the bulk pressure P [in units of $\hbar^2/(2ma^2n)$], and the sound velocity c_s [in units of $[\hbar^2/(2m^2a^2)]^{1/2}$].

wave-number branch (linear part) of the spectrum $\omega(k)$ of the elementary excitations. Unfortunately, the imaginary-time formulation of PIGS method prevents us from obtaining the exact dynamical properties of the system, such as the full excitation spectrum $\omega(k)$, directly from simulations. Some features of $\omega(k)$ can be obtained within the Feynman's approximation:

$$\hbar\omega(k) = \frac{\hbar^2 k^2}{2mS(k)}, \tag{19}$$

where

$$S(k) = \frac{1}{N}\left\langle \sum_{j=1}^{N} e^{-i\vec{k}\cdot\vec{r}_j} \sum_{l=1}^{N} e^{i\vec{k}\cdot\vec{r}_l} \right\rangle \tag{20}$$

is the static structure factor that can be readily obtained during a PIGS simulation. Our results for the Feynman's excitation spectrum for HS at different values of the gas parameter are reported in Fig. 6. The Feynman's approximation is known to be accurate only at very low na^3, and to become only qualitative at higher values of the gas parameter. For example, in the case of superfluid ^{4}He, where $na^3 = 0.244$, it overestimates the roton minimum by a factor of about 2. In the low wave-vector limit we find that, in spite of the well-known size effect on the static structure factor (20) [23], Feynman's approximation turns out to be in a remarkable agreement with the phononic dispersion (18) with the values of the sound velocity c_s given by Eq. (17) and reported in Fig. 5. It is worth noting that even Feynman's approximation (19) for the excitation spectrum, as the energy per particle and the condensate fraction, deviates from the Bogoliubov approximation for $na^3 \simeq 10^{-3}$. Another remarkable feature is that, even within this simple approximation, the occurrence of a roton minimum at high density is correctly described.

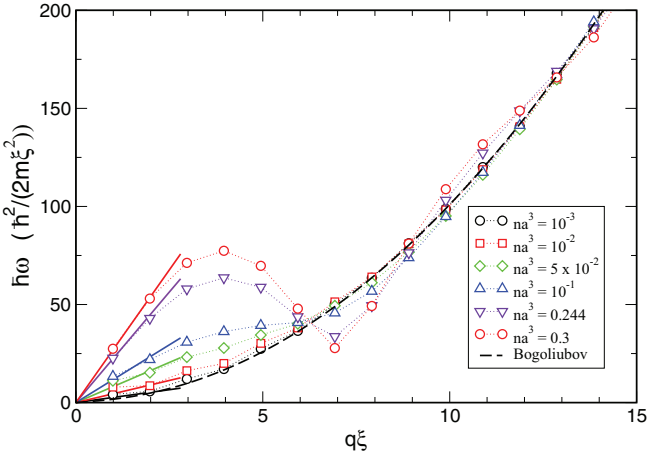

FIG. 6. (Color online) Excitation spectrum obtained with Feynman's approximation at different values of the gas parameter na^3. Dotted lines are given as guides to the eye. In order to make comparable results at different na^3 the spectra are plotted as a function of $q\xi$ and in units of $\hbar^2/2m\xi^2$, where $\xi = an^{1/3}$. In these units, the Bogoliubov approximation for the excitation spectrum (dashed line) reads $\hbar\omega(q) = \sqrt{(q\xi)^4 + 2(q\xi)^2}$. The relative low wave-vector phononic dispersion, Eq. (18), are reported as straight lines.

V. INCLUSION OF A TRAPPING HARMONIC POTENTIAL

We consider now the effect of confinement due to an external anisotropic harmonic potential

$$U(\mathbf{r}) = \frac{m}{2}[\omega_\perp(x^2 + y^2) + \omega_z z^2], \tag{21}$$

where $\omega_\perp$ is the cylindric radial frequency and ω_z is the cylindric longitudinal frequency. The collective dynamics of the system can be described efficiently by the hydrodynamic equations, modified by the inclusion of the external potential $U(\mathbf{r})$ [2,3], namely

$$\frac{\partial n}{\partial t} + \nabla\cdot(n\mathbf{v}) = 0, \tag{22}$$

$$m\frac{\partial \mathbf{v}}{\partial t} + \nabla\left[\frac{1}{2}mv^2 + \mu[n,a] + U(\mathbf{r})\right] = \mathbf{0}. \tag{23}$$

It has been shown in Ref. [24] that by assuming a power-law dependence $\mu = \mu_0 n^\gamma$ for the chemical potential (polytropic equation of state) from Eqs. (14) and (15) one finds analytic expressions for the collective frequencies. In particular, for very elongated cigar-shaped traps ($\omega_\rho/\omega_z \gg 1$) the collective radial breathing mode frequency Ω_ρ is given by

$$\Omega_\rho = \sqrt{2(\gamma+1)}\omega_\rho, \tag{24}$$

while the collective longitudinal breathing mode Ω_z is

$$\Omega_z = \sqrt{\frac{3\gamma+2}{\gamma+1}}\omega_z. \tag{25}$$

In our problem we introduce an effective polytropic index γ as the logarithmic derivative of the chemical potential μ, that is

$$\gamma = \frac{n}{\mu}\frac{\partial\mu}{\partial n} = \frac{2xf_g'(x) + x^2 f_g''(x)}{f_g(x) + xf_g'(x)}, \tag{26}$$

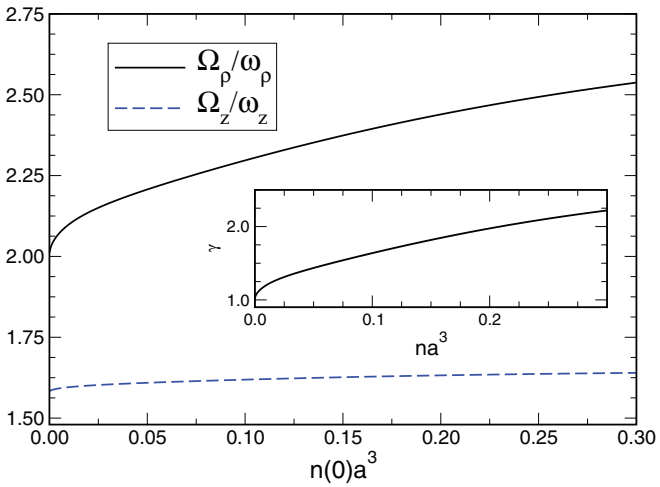

FIG. 7. (Color online) Breathing mode frequencies of the Bose gas of HS under strong anisotropic axially symmetric harmonic confinement. Ω_ρ is the frequency of the radial breathing mode and Ω_z is the frequency of the axial breathing mode. Here $n(0)a^3$ is the local gas parameter with $n(0)$ the gas density at the center of the trap. Inset: effective polytropic index γ as a function of the gas parameter.

where $f_g(x)$ is given by Eq. (5). This approach has been very successful [12] in the study of the experimentally observed [25] breathing modes of a two-component Fermi gas of ^{6}Li atoms in the BCS-BEC crossover. Indeed, in Ref. [12] we have suggested relevant deviations to the mean-field results, which have been subsequently confirmed by improved experiments [26].

In Fig. 7 we report the frequencies Ω_ρ and Ω_z of breathing modes as a function of the gas parameter $n(0)a^3$, where $n(0)$ is the density at the center of the strongly anisotropic harmonic trap. The figure shows a relevant change in the scaled radial frequency Ω_ρ/ω_ρ that is a direct consequence of the fact that the effective polytropic index γ increases from $\gamma \simeq 1$ in the weak-coupling regime to $\gamma \simeq 2.2$ in the strong-coupling regime as shown in the inset of Fig. 7.

VI. CONCLUSIONS

The properties of bulk systems of HS for a wide range of the gas parameter na^3, going from the dilute gas to the solid phase, have been investigated with the exact $T = 0$ PIGS Monte Carlo methods. Our results for the energy per particle turn out to be in good agreement with previous calculations, performed with different Monte Carlo techniques, in the gas parameter range in which they were available [4,5]. We have found that recent beyond mean-field approximations are compatible with our Monte Carlo data up to $na^3 \simeq 10^{-3}$.

We have then fitted our PIGS data via polynomials functions, Eqs. (5) and (7), which have been then used to locate the gas-liquid transition with a standard Maxwell construction. Our analytical fit extends the range of applicability of the previous equation of state [20] up to the freezing point, and beyond it in the metastable region. We have computed also the condensate fraction n_0/n in the whole considered gas parameter range. In particular, we have found that the condensate fraction is zero in the solid phase, in agreement with what happens in the solid phase of systems interacting with more realistic potentials such as ^{4}He [16,18]. We have provided an analytical fit also for n_0/n showing that, as in Ref. [5], the Bogoliubov approximation overestimates the condensate fraction for na^3 larger than 10^{-3}, while the recent improved perturbative approach of Ref. [21] extends the predictive region of mean-field approaches of about an order of magnitude, up to $na^3 \simeq 10^{-2}$.

The fit of PIGS data are useful in order to derive other relevant properties of the bulk system, such as the chemical potential and the pressure. By means of the zero-temperature hydrodynamics equations of superfluids it is indeed possible to obtain other relevant physical quantities. In particular, we have calculated the sound velocity for gas parameters up to 0.3. This is relevant also because PIGS cannot give direct access to dynamical properties of the system. Some qualitative information about the excitation spectrum can be recovered via Feynman's approximation: the low-wave-vector limit of such an approximate spectrum agrees with the linear phononic dispersion obtained from the hydrodynamic equation of superfluids (14) and (15) with the equation of state (5). More quantitative results on the excitation spectrum can be obtained by computing the intermediate scattering functions via PIGS and then by analytically continuing them with inversion methods, like GIFT [27], for example, in order to recover the dynamical structure factor. These procedures are typically laborious and require a large amount of computations, and they go beyond the aim of this paper; anyway, while writing this paper, we became aware that a similar study is under investigation [28]. It is worth noting, however, that even in an approximate fashion, also an approximation as simple as Feynman's is able to capture the emerging of the phonon-roton spectrum deduced by Landau [29] with the increasing gas parameter.

Finally, we have shown that analytical expressions of the exact equation of state can be useful also for predictions in confined systems. The hydrodynamic equations can be used to calculate density profiles and collective modes in various trap configurations [2,3]. Here we have derived the frequencies of the collective breathing modes of an HS gas confined in a strongly anisotropic harmonic trap as a function of the local gas parameter. By including a gradient correction in the hydrodynamic equations one can rewrite them as a nonlinear Schrödinger equation (generalized Gross-Pitaevskii equation) [30,31] and study other fundamental properties like quantized vortices [31], solitons [32], and shock waves [33].

ACKNOWLEDGMENTS

The authors thank F. Ancilotto, D. E. Galli, R. Rota, and F. Toigo for useful discussions. The authors acknowledge for partial support Università di Padova (Research Project "Quantum Information with Ultracold Atoms in Optical Lattices"), Cariparo Foundation (Excellence Project "Macroscopic Quantum Properties of Ultracold Atoms under Optical Confinement"), and Ministero Istruzione Università Ricerca (PRIN Project "Collective Quantum Phenomena: from Strongly-Correlated Systems to Quantum Simulators").

[1] J. P. Hansen and I. R. McDonalds, *Theory of Simple Fluids*, 3rd ed. (Academic Press, London, 2006).
[2] L. P. Pitaevskii and S. Stringari, *Bose-Einstein Condensation* (Oxford University Press, Oxford, 2003).
[3] A. J. Leggett, *Quantum Liquids. Bose Condensation and Cooper Pairing in Condensed-Matter Systems* (Oxford University Press, Oxford, 2006).
[4] M. H. Kalos, D. Levesque, and L. Verlet, Phys. Rev. A **9**, 2178 (1974).
[5] S. Giorgini, J. Boronat, and J. Casulleras, Phys. Rev. A **60**, 5129 (1999).
[6] H. Kim, C. S. Kim, C. L. Huang, H. S. Song, and X. X. Yi, Phys. Rev. A **85**, 053629 (2012).
[7] L. M. Sesé, J. Chem. Phys. **139**, 044502 (2013).
[8] K. J. Runge and G. V. Chester, Phys. Rev. B **38**, 135 (1988).
[9] L. M. Sesé and R. Ledesma, J. Chem. Phys. **102**, 3776 (1995).
[10] L. M. Sesé, J. Chem. Phys. **108**, 9086 (1998).
[11] A. Sarsa, K. E. Schmidt, and W. R. Magro, J. Chem. Phys. **113**, 1366 (2000).
[12] N. Manini and L. Salasnich, Phys. Rev. A **71**, 033625 (2005).
[13] D. M. Ceperley, Rev. Mod. Phys. **67**, 279 (1995).
[14] J. Cao and B. J. Berne, J. Chem. Phys. **97**, 2382 (1992).
[15] M. Rossi, M. Nava, D. E. Galli, and L. Reatto, J. Chem. Phys. **131**, 154108 (2009).
[16] E. Vitali, M. Rossi, F. Tramonto, D. E. Galli, and L. Reatto, Phys. Rev. B **77**, 180505(R) (2008).
[17] M. Boninsegni, J. Low Temp. Phys. **141**, 27 (2005).
[18] M. Boninsegni, N. Prokof'ev, and B. Svistunov, Phys. Rev. Lett. **96**, 070601 (2006); M. Boninsegni, N. V. Prokof'ev, and B. V. Svistunov, Phys. Rev. E **74**, 036701 (2006).
[19] T. D. Lee, K. Huang, and C. N. Yang, Phys. Rev. **106**, 1135 (1957).
[20] J. Boronat, J. Casulleras, and S. Giorgini, Physica B **284–288**, 1 (2000).
[21] V. I. Yukalov and E. P. Yukalova, Phys. Rev. A **74**, 063623 (2006).
[22] J. P. Hansen, D. Levesque, and D. Schiff, Phys. Rev. A **3**, 776 (1971).
[23] E. W. Draeger and D. M. Ceperley, Phys. Rev. B **61**, 12094 (2000).
[24] M. Cozzini and S. Stringari, Phys. Rev. Lett. **91**, 070401 (2003).
[25] M. Bartenstein, A. Altmeyer, S. Riedl, S. Jochim, C. Chin, J. H. Denschlag, and R. Grimm, Phys. Rev. Lett. **92**, 203201 (2004).
[26] A. Altmeyer, S. Riedl, C. Kohstall, M. J. Wright, R. Geursen, M. Bartenstein, C. Chin, J. H. Denschlag, and R. Grimm, Phys. Rev. Lett. **98**, 040401 (2007).
[27] E. Vitali, M. Rossi, L. Reatto, and D. E. Galli, Phys. Rev. B **82**, 174510 (2010).
[28] R. Rota, F. Tramonto, D. E. Galli, and S. Giorgini, arXiv:1310.1753.
[29] L. D. Landau, J. Phys. USSR **11**, 91 (1947).
[30] L. Salasnich, Laser Phys. **19**, 642 (2009).
[31] S. K. Adhikari and L. Salasnich, Phys. Rev. A **77**, 033618 (2008).
[32] L. Salasnich, A. Parola, and L. Reatto, J. Phys. B **39**, 2839 (2006).
[33] B. Damski, Phys. Rev. A **69**, 043610 (2004); L. Salasnich, Europhys. Lett. **96**, 40007 (2011).